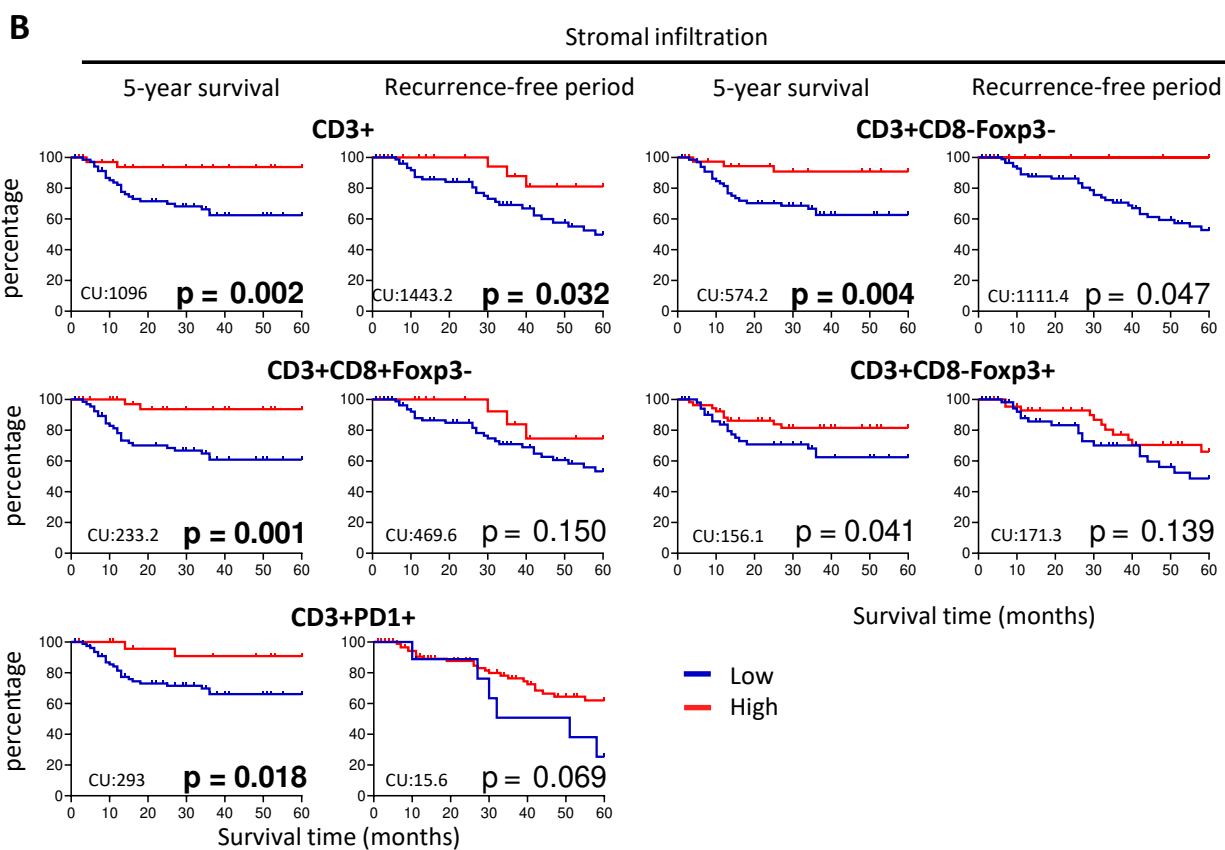
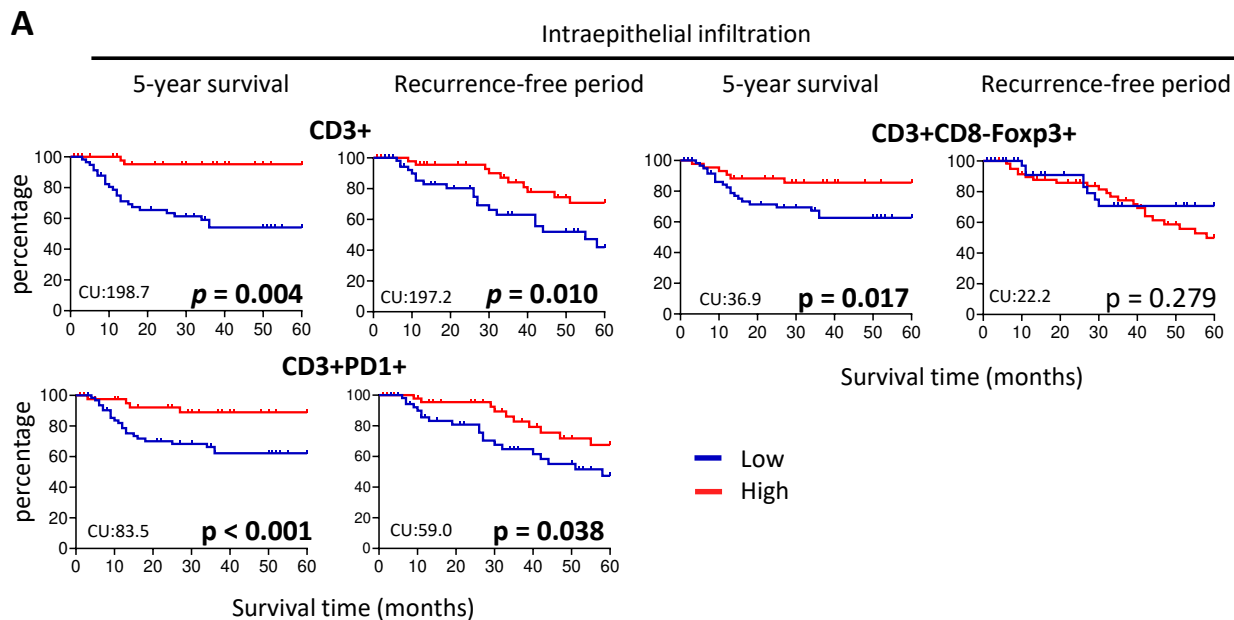
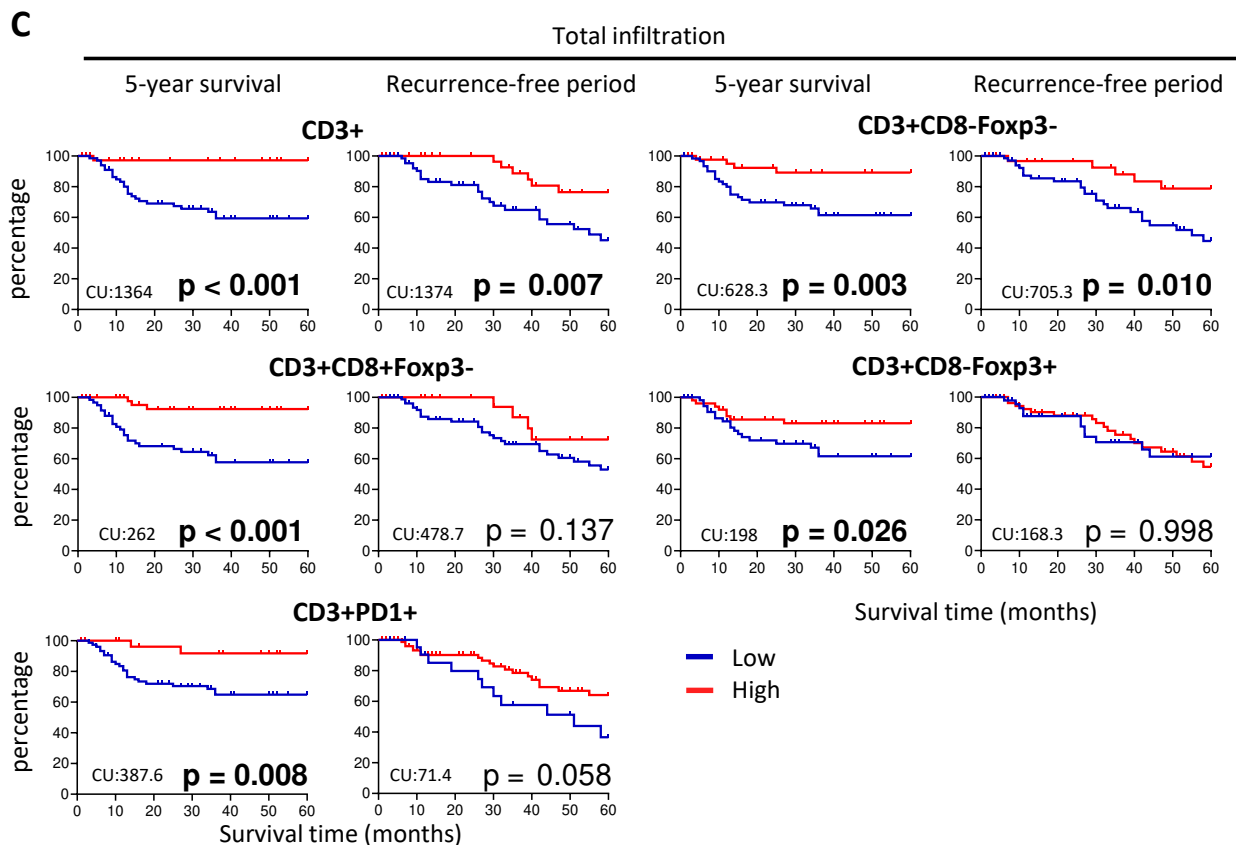
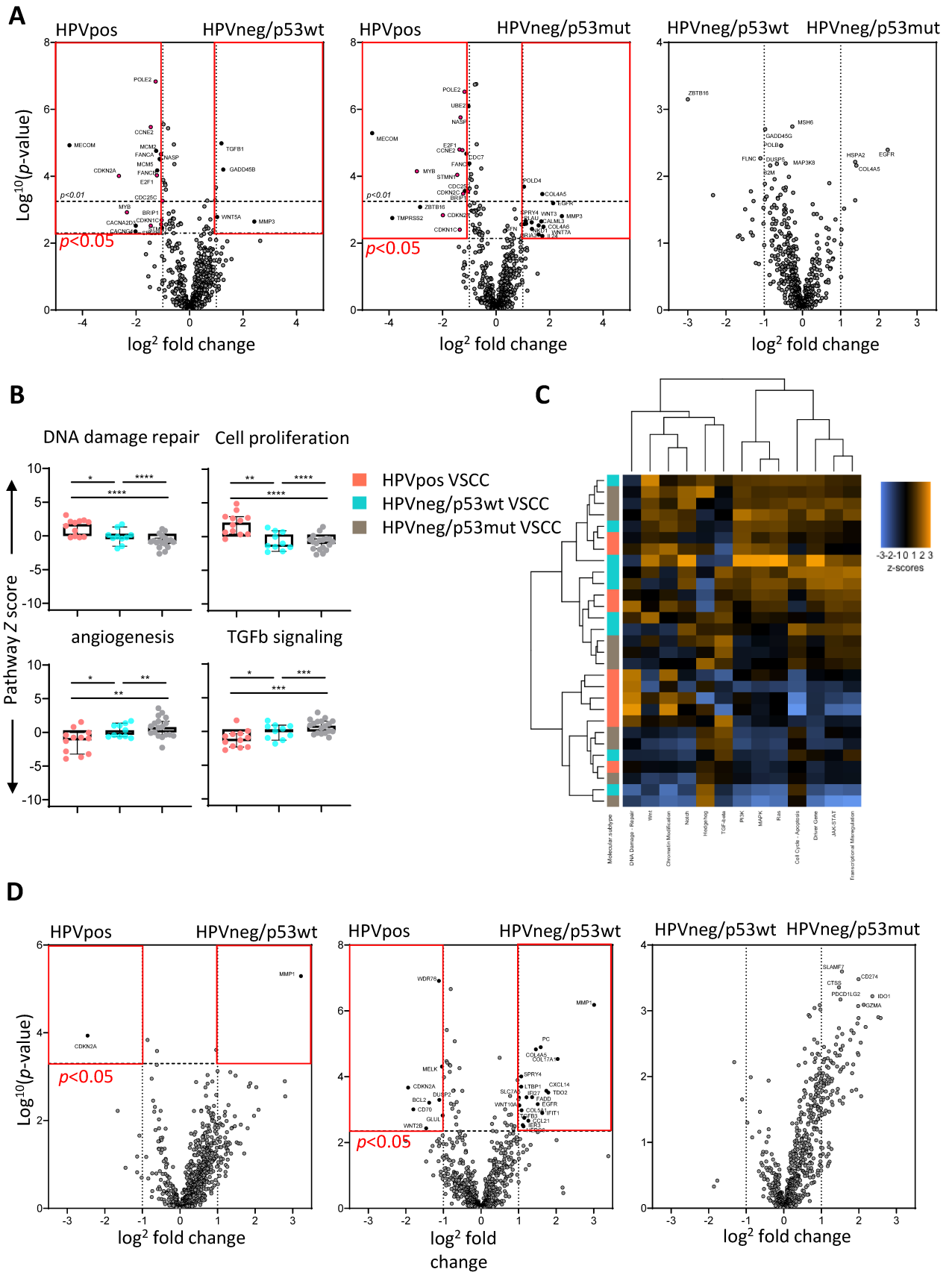


Supplemental figure 1. Low and high infiltrated tumors were categorized based on their intraepithelial CD3⁺ cell count. Paraffin-embedded tumor tissue of VSCC patients was analyzed by multiplex immunofluorescent VECTRA analysis with antibodies directed against CD3, CD8, Foxp3, PD-1, pan-cytokeratin and DAPI as described in reference 9. **A**) Scatter plot displaying the number of intraepithelial CD3⁺ T cell counts/mm² for patients with low infiltration (i.e. deserted (D; blue) and altered-immunosuppressed (AI, green)) or high infiltration (i.e. altered-excluded (AE, orange) and inflamed (I; red)) VSCC for the 109 FIGO I-III VSCC. **B, C**) Bar graphs displaying the observed T cell infiltration patterns for early-stage (black) and late-stage (grey) VSCC (**B**) and total cohort of VSCC (**C**). **D**) Kaplan-Meier curves showing 5-year survival (left) and the recurrence free period (RFP; right) for 109 FIGO I-III VSCC patients with inflamed (red; n=14), altered-excluded (orange; n=37), altered-immunosuppressed (green; n=26) and deserted (blue; n=32) T-cell infiltration patterns. Statistical significance of the survival distribution was analyzed by log-rank testing (Mantel-Cox and trend), and differences were considered significant when $p < 0.05$.

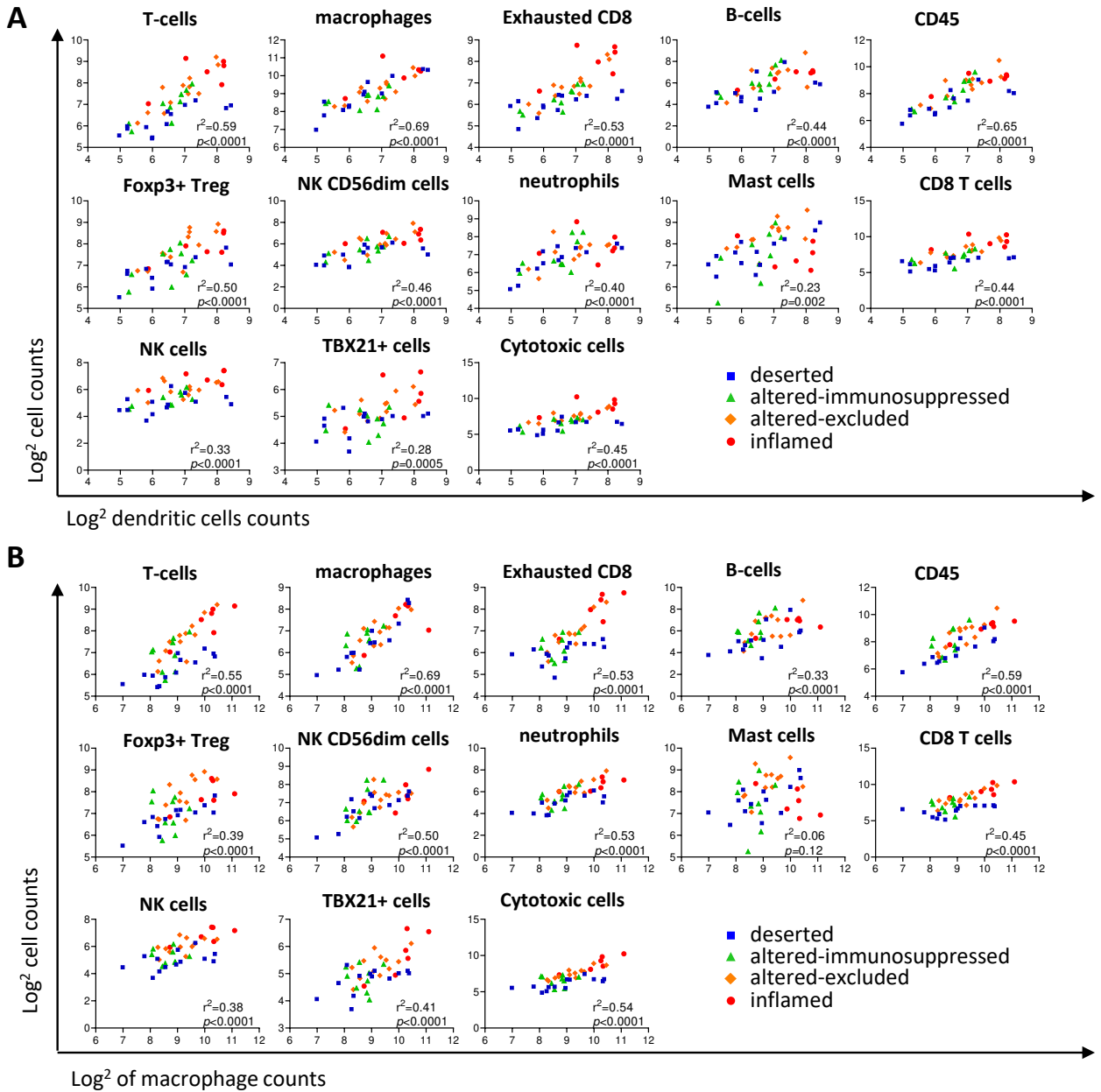




Supplemental Figure 2. High immune infiltration is associated with better clinical outcome. Kaplan-Meier curves showing the 5-years overall survival (first and third column) and recurrence-free period (second and fourth column) for early- and late-stage VSCC patients with low (blue) or high (red) numbers of **A**) intraepithelial CD3+, CD3+CD8-Foxp3+ and CD3+PD1+ cells/mm² and of stromal **B**) and total **C**) CD3+, CD3+CD8-Foxp3-, CD3+CD8-Foxp3+, CD3+CD8-Foxp3+, and CD3+PD1+ cells/mm². Patients were grouped into the low or high groups based on the best cut-off value (CU) for each subset as determined by receiver operating characteristics (ROC) curve analysis. Patients with a T cell count below the cut-off value were classified as low, and visa versa. CU values are given in the low left corner of each Kaplan-Meier curve. Statistical significance of the survival distribution was analyzed by log-rank testing. Significant differences $p < 0.05$ were shown in bold.

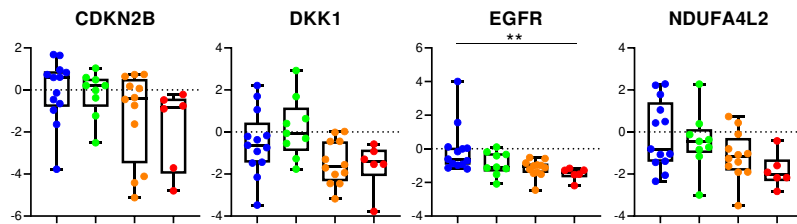


Supplemental figure 3. Minor differences observed between molecular subtypes of VSCC. Early-stage (n=29) and late-stage (n=11) VSCC of all three molecular subtypes (HPVpos (n=12), HPVneg/p53wt (n=10), and HPVneg/p53mut (n=18) VSCC) were analyzed by the PanCancer oncogenic pathway (early-stage only) and PanCancer IO360 (early- and late-stage) panels. The data were analyzed using nCounter Advanced Analysis module 2.0 software. **A)** Volcano plots depicting the differentially expressed genes (DEGs) between HPVpos and HPVneg/p53wt (left), HPVpos and HPVneg/p53mut (middle) and HPVneg/p53wt and HPVneg/p53mut (right) early-stage VSCC based on a \log^2 fold change of >1 or <-1 in combination with Benjamini-Hochberg (BH) adjusted $p < 0.05$. Significant (BH p-values) genes are indicated by the red lines. Overlapping DEGs that are up in HPVpos vs HPVneg/p53wt or HPVneg/p53mt are indicated in pink. **B)** Box plots showing the differences in the cancer-associated canonical signaling pathways Z scores for HPVpos (red), HPVneg/p53wt (blue) and HPVneg/p53mut (grey) VSCC. **C)** Heatmap plot displaying pathway scores of 13 cancer-associated canonical signaling pathways within the PanCancer Pathway panel. Pathway scores were calculated and displayed as Z-transformed values where orange represents high scores, and blue represents low scores. **D)** Volcano plots depicting the differentially expressed genes (DEGs) between HPVpos and HPVneg/p53wt (left), HPVpos and HPVneg/p53mut (middle) and HPVneg/p53wt and HPVneg/p53mut (right) early-stage and late-stage VSCC based on a \log^2 fold change of >1 or <-1 in combination with Benjamini-Hochberg (BH) adjusted $p < 0.05$. Significant (BH p-values) genes are indicated by the red lines. * $p < 0.05$, ** $p < 0.01$, *** $p < 0.001$, and **** $p < 0.0001$.

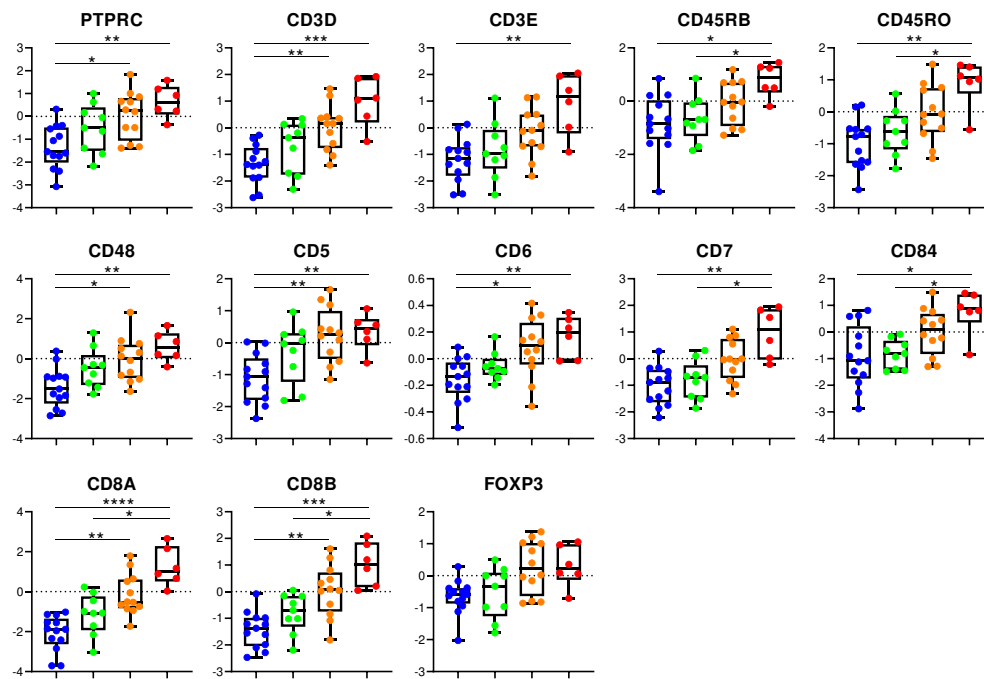


Supplemental figure 4. A coordinated immune response between immune cell types. Automated cell type profiling was performed by using nCounter Advanced Analysis module 2.0 software and was based on the expression of pre-defined genes (Supplemental Table 4). Linear regression analyses of indicated deconvoluted cell types (Y-axis) versus **A**) dendritic cells (DCs, X-axis) and **B**) macrophages (X-axis). Data is given as log₂ transformed cell counts. The different T-cell infiltration patterns are depicted in color code. * $p < 0.05$, ** $p < 0.01$, *** $p < 0.001$, and **** $p < 0.0001$.

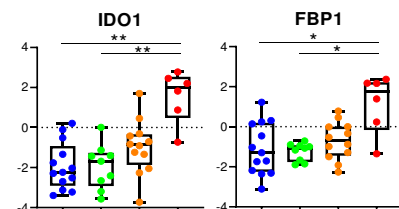
Upregulated in cold



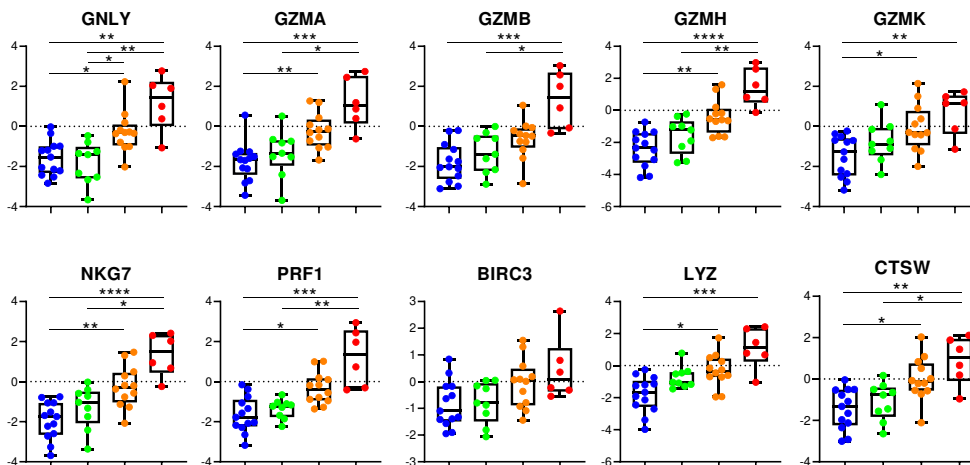
Lymphoid compartment



Myeloid compartment

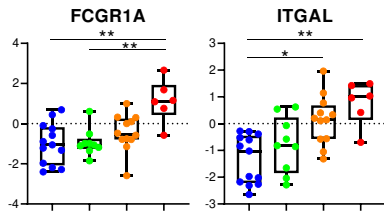


cytotoxicity

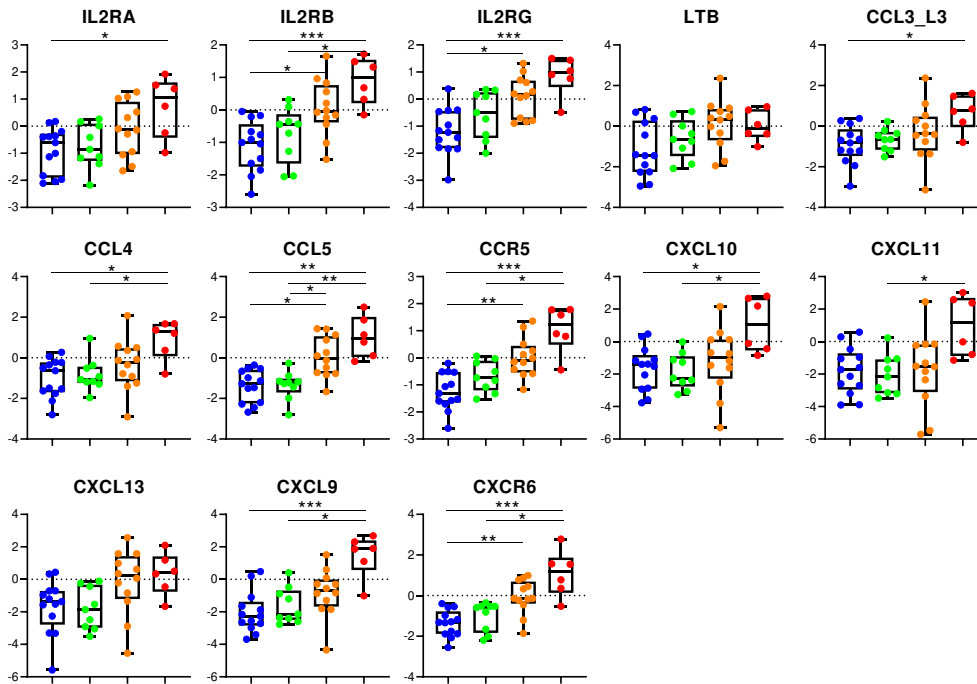


Supplemental figure 5

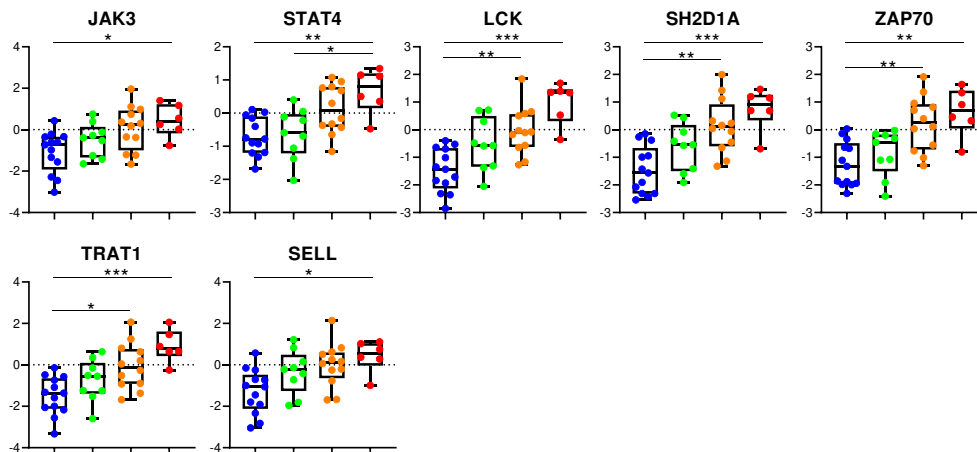
Adhesion and migration



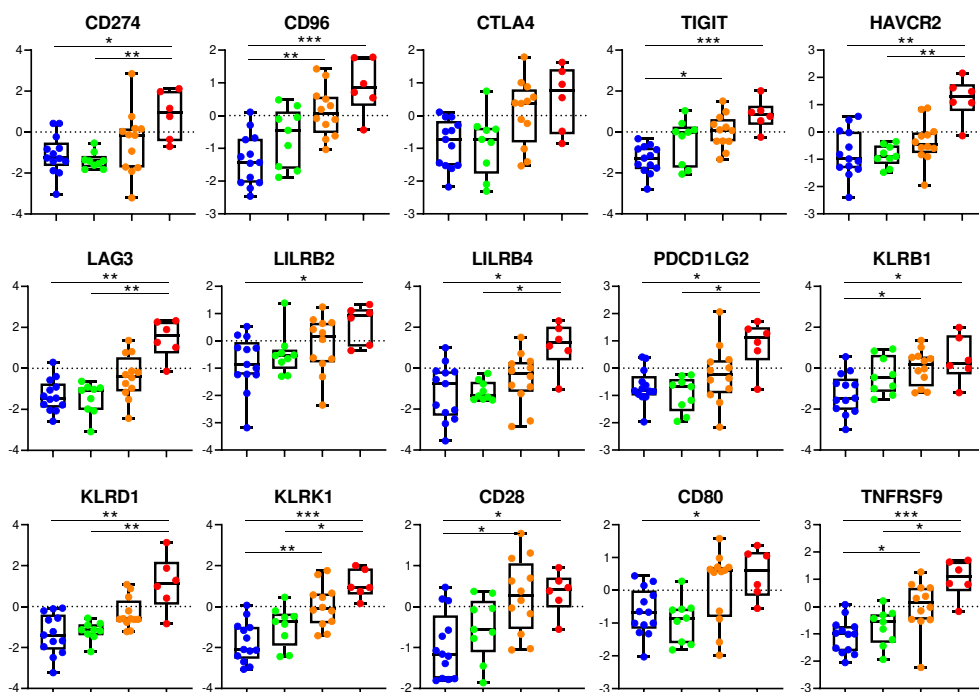
Cytokine and chemokine signaling



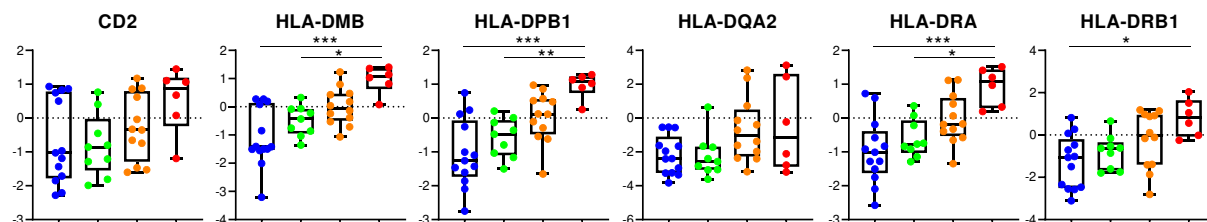
T cell signaling



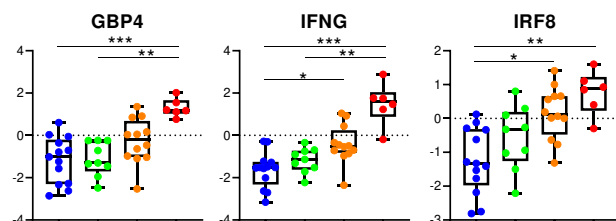
Checkpoint molecules



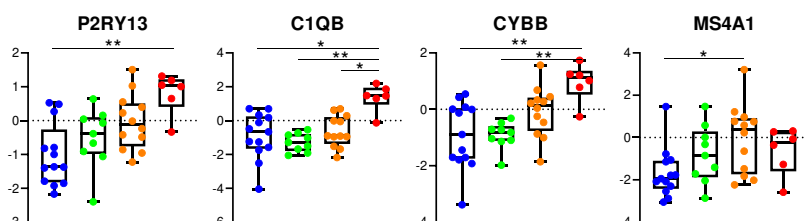
Antigen presentation



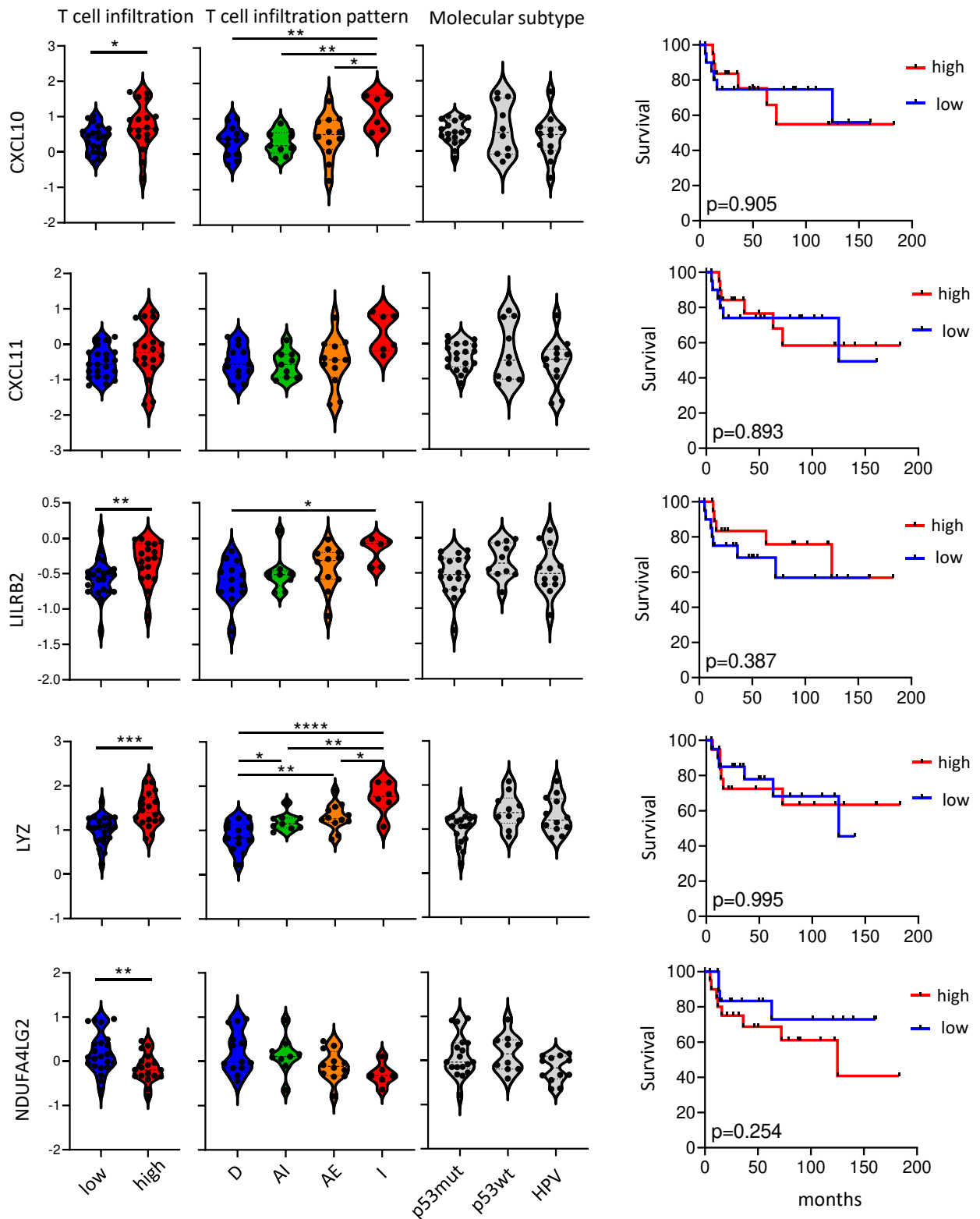
IFN signaling



miscellaneous



Supplemental figure 5. All differentially expressed single genes that were different between high and low infiltrated tumors were depicted in respect to their T cell infiltration pattern. Box plots displaying all significant differentially expressed genes (corrected p -value <0.05 and \log^2 fold change >1 or <-1) between high and low infiltrated tumors. Expression of the selected single genes in the heatmap were given as \log^2 transformed values relative to the average value of that particular gene. VSCC patients are categorized based on the T-cell pattern: deserted (blue), altered-immunosuppressed (green), altered-excluded (orange) and inflamed (red). * $p<0.05$, ** $p<0.01$, *** $p<0.001$, and **** $p<0.0001$.



Supplemental figure 6. High infiltrated tumors are associated with a higher VSCC-inflamed gene expression profile (GEP) score. Forty VSCC samples of all three molecular subtypes (HPVpos, HPVneg/p53wt and HPVneg/p53mut VSCC) were analyzed by the Nanostring IO360 Pancancer panel, and log₁₀ transformed expression values for *CXCL10*, *CXCL11*, *LILRB2*, *LYZ* and *NDUFA4LG2* were determined. Graphs depict violin plots and Kaplan-Meier survival curves for the individual genes. Violin plots display the log₁₀-transformed expression values for T cell infiltration (low versus high tumors), T cell infiltration pattern (deserted (D), altered-immunosuppressed (AI), altered-excluded (AE) and Inflamed (I) VSCC) and tumor molecular subtype (HPVneg/p53mut, HPVneg/p53wt and HPVpos VSCC). Kaplan-Meier survival curves showing the survival of 40 VSCC patients with high (red; above the median) and low (blue; below the median) expression of the indicated genes. * $p < 0.05$, ** $p < 0.01$, *** $p < 0.001$, and **** $p < 0.0001$.